An Experimental Study on Vibration Isolation Performance of Weft-Knitted Spacer Fabrics

Fuxing Chen, Yanping Liu, Hong Hu

Institute of Textiles and Clothing, The Hong Kong Polytechnic University, Hung Hom, Hong Kong

ABSTRACT: This paper presents an experimental study on the vibration isolation performance of weft-knitted spacer fabrics under forced harmonic excitation. The weft-knitted spacer fabrics with two different thicknesses were first designed by varying the linking distance of spacer monofilament and fabricated using an electronic flat knitting machine. Then, their vibration isolation performance was tested under forced vibration condition via sinusoidal sweeps from low to high frequencies. The typical acceleration transmissibility curve and effects of fabric thickness, load mass and excitation level were discussed in detail. The results obtained show that the thicker spacer fabric has lower resonance frequency than thinner fabric due to lower stiffness, and thus can isolate the vibration at a lower frequency level. The results also show that changing the load mass and excitation level changes the loading conditions of the fabric structure, and thus also changes fabric stiffness and vibration isolation performance due to nonlinear behavior of spacer fabrics. It is expected that this study could provide some useful information to promote the application of weft-knitted spacer fabrics for vibration isolation.

Keywords: Spacer fabric, stiffness, vibration isolation, resonance frequency

INTRODUCTION

Human body is sensitive to vibrational environments coming from electrical and pneumatic

powered rotary tools and processes in mining, quarrying, demolition and road construction [1], which may cause discomfort and disease. For example, workers with considerable exposure to hand-transmitted vibrations may develop hand arm vibration syndromes (HAVS) such as vibration-induced white finger (VWF) and peripheral neurological disorders. To buffer vibration effects on the human body, passive anti-vibration materials such as rubber and polyurethane foams have been made into car cushions, anti-vibration gloves and so on. [2-5] However, these conventional anti-vibration materials are not very comfortable due to their low air and moisture management. Knitted spacer fabrics could be an alternative choice for vibration isolation because they can provide better thermophysiological comfort for the human body.

Knitted spacer fabrics are a type of sandwiched textile structure consisting of two outer layers that are connected but kept apart by a spacer layer of monofilaments. Because of this structural feature, knitted spacer fabrics have been developed for a number of applications such as compression bandages and wound dressings [6-10], sound attenuation [11, 12], concrete reinforcement [13, 14], geotextiles [15, 16], solar thermal insulation [17], impact protection [18-20] and piezoelectric effect for energy harvesting [21]. Knitted spacer fabrics with unusual behaviors such as negative Poisson's ratio [22-24] and negative stiffness [25] have also been developed. There is no doubt that knitted spacer fabrics can also be developed to reduce the magnitudes of sportive and occupational vibrations due to their versatility and good mechanical performance. However, relevant studies are still very limited.

At present, there have been very few studies conducted on the vibration properties and isolation performance of knitted spacer fabrics. Blaga et al. [26, 27] used impact tests to study the dynamic

response of both warp- and weft-knitted spacer fabrics along different fabric directions based on the transmissibility curves obtained from the fast Fourier transform. Arabzadeh et al. [28] built mathematical models for the free vibration of multi-layer warp-knitted spacer fabrics under impact force. They found that decreasing the fineness and length of monofilaments and increasing their density could increase the transmitted force. Liu and Hu [29] studied the vibration isolation properties of warp-knitted spacer fabric top-loaded with a mass, and found that the resonance frequency measured by vibration test matched with the quasi-static compression curve. However, these studies were mostly focused on warp-knitted spacer fabrics. Until now, studies on the vibration isolation performance of weft-knitted spacer fabrics are still needed.

This paper presents an experimental study on the vibration isolation performance of weft-knitted spacer fabric under forced harmonic excitation. Compared with warp-knitted spacer fabrics, weft-knitted fabrics have a greater extensibility and can better conform to the shape of an object due to the loop nature of weft-knitted stitches. In addition, elastic yarns can be easily used for knitting weft-knitted spacer fabrics to increase fabric elasticity. As a result, they are more suitable for producing products for vibration isolation such as anti-vibration gloves. On the other hand, it is well known that the main approach to achieving good vibration isolation is to reduce the dynamic stiffness of isolation material. Previous studies [25, 30] have already shown that a thicker weft-knitted spacer fabric has lower stiffness. Hence, to reduce the stiffness of weft-knitted spacer fabrics for obtaining a low resonance frequency in vibration isolation, the use of thicker spacer fabrics is recommended. However, the thickness of weft-knitted spacer fabrics is usually low due to the limitation in adjusting the distance between two needle systems in a weft knitting machine. Therefore, relatively thick knitted spacer fabrics are realized by a proper fabric

design in this study. In order to test the vibration isolation performance of these spacer fabrics, a vibration test system with a mass loaded on the upper layer of spacer fabric was used. The effects of different factors such as fabric thickness, load mass and excitation level on the vibration transmissibility of the mass-spacer fabric system were discussed. It is expected that this study could strengthen the understanding of the vibration behavior of weft-knitted spacer fabrics, and provide some useful information to promote their applications in anti-vibration.

PREPARATION OF FABRIC SAMPLES

Design of fabric structure

Due to the limited distance between two needle systems in a weft knitting machine, a special fabric structure was first suggested to fabricate thicker weft-knitted spacer fabrics by employing longer linking distance of spacer monofilaments to knit the spacer layer and elastic yarns to knit the outer layers in this study. As shown in Figure 1(a), the suggested spacer structure is constructed of two outer layers knitted with elastic yarns in single jersey and a spacer layer knitted with tuck loops using monofilaments in "X" shape. As the outer layers are knitted with elastic yarns, they will shrink after a steaming treatment, causing the inclined monofilaments rotated to the thickness direction of the fabric structure and thus making the fabric thickness increased, as shown in Figure 1(b). If different linking distances of spacer monofilaments are adopted, spacer fabrics with different thicknesses can be easily realized. Actually, this design concept has been used in the development of spacer fabrics with negative stiffness [25].

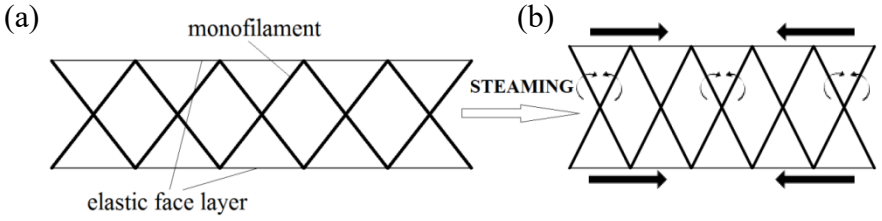

Figure 1 Design concept of weft-knitted spacer fabric structure: (a) before steaming treatment; (b) after steaming treatment.

In order to obtain the spacer fabric as thick as possible, a linking distance of 20 needles, which is a maximum distance for a normal knitting process, was first selected after a series of preliminary trials, as shown in Figure 2(a). Beyond this distance, knitting becomes very difficult as needles for tucking could not well catch monofilaments, causing knitting defects. On the other hand, in order to study the effect of the fabric thickness, the linking distance was reduced to 12 needles to obtain a thinner spacer fabric but still having sufficient thickness for good vibration isolation for comparison, as shown Figure 2(b). The two fabric structures were named as Spacer-20h and Spacer-12h, where the number indicates the floating distance of each monofilament between two tucking points on the same needle bed, and "h" indicates only half numbers of needles knitting tuck stitches. From Figure 2, it can be seen that the tuck positions are evenly distributed. It should be pointed out that as the cross-over structure of the spacer monofilaments in "X" shape along the course direction makes fabric structure balanced under compression loads, the transverse shift along the courses of fabric does not arise. It is possible to let all needles knit tuck stitches. However, twofold monofilaments limit the shrinkage of the outer layers during the steaming treatment, resulting in relatively low fabric thickness which limits the range of displacement under vibration. Therefore, the structure with all needles knitting tuck stitches was not adopted in this study.

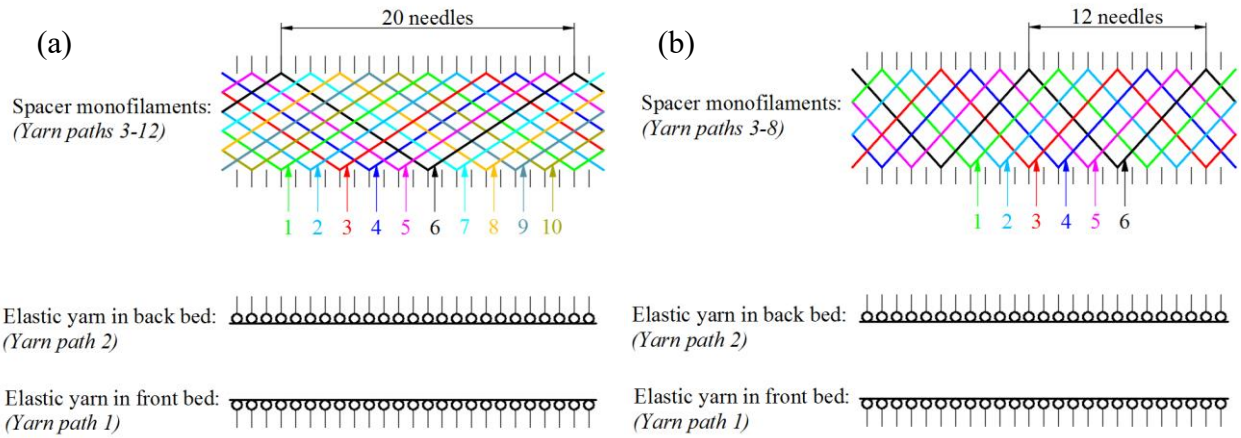

Figure 2 Fabric structures with different linking distance of spacer monofilaments: (a) Spacer-20h; (b) Spacer-12h.

Fabrication of fabric samples

The above proposed fabrics were knitted on a 14 gauge STOLL CMS 822 computerized flat knitting machine. While the two outer layers were knitted with single jersey structure using one 100D nylon multifilament yarn and one 30D Spandex/70D nylon covering yarn together, the spacer layer was knitted with 0.12 mm polyester monofilament. The NP value, which refers to cam setting, was set at 9.0 for knitting the spacer layer, and 11.0 for knitting two outer layers, respectively. After knitting, fabric samples at their free state were subjected to a steaming treatment with a steam iron. The temperature of the steam iron was kept at around 50℃ to avoid possible yarn damages. Elastic yarns in the outer layers shrank during the steaming treatment, resulting in fabric thickening. After the steaming treatment, the fabric samples were further relaxed under an environmental condition of 20℃ and 65% RH for one week. The characteristics of two fabric samples Spacer-20h and Spacer-12h after relaxation are listed in Table 1. It can be seen that the loop densities of two fabrics are similar, but Spacer-20h has greater areal mass and fabric thickness than Spacer-12h.

Table 1 The characteristics of two weft-knitted spacer fabrics.

Fabric code	Course density (wales/cm)	Wale density (courses/cm)	Areal mass (g/m^2)	Thickness (mm)
Spacer-20h	7.15 (0.12)	26.10 (0.91)	1020.15 (21.99)	12.01 (0.17)
Spacer-12h	6.66 (0.06)	25.90 (0.42)	673.27 (31.33)	6.66 (0.18)

Note: Standard deviations are given in parentheses.

Figure 3 shows the cross-sectional views of the as-fabricated weft-knitted spacer fabrics. It can be found that the cross-sectional views along the course direction and the wale direction are different. Along the course direction, spacer monofilaments have a crossed structure. However, along the wale direction, spacer monofilaments have a curved shape. Moreover, linking points A and B of each monofilament with two outer layers are not located on the same vertical line. This dislocation between A and B should be taken into consideration when preparing the fabric samples for vibration testing.

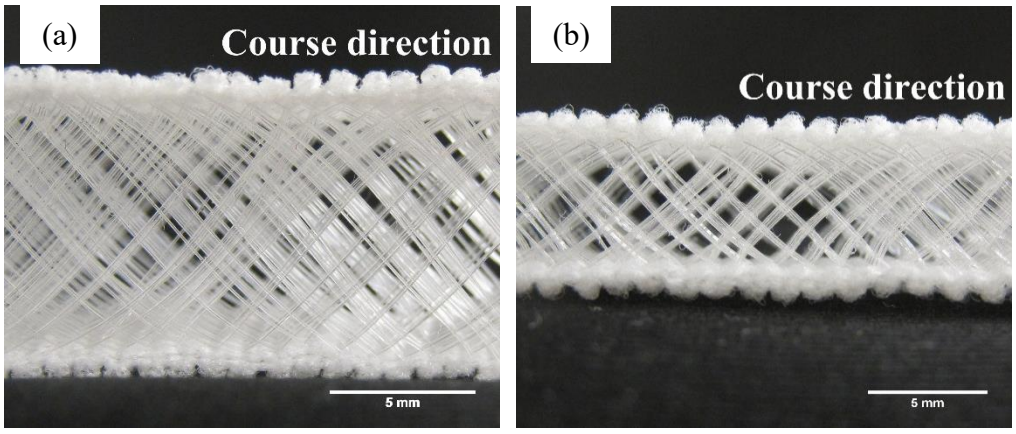

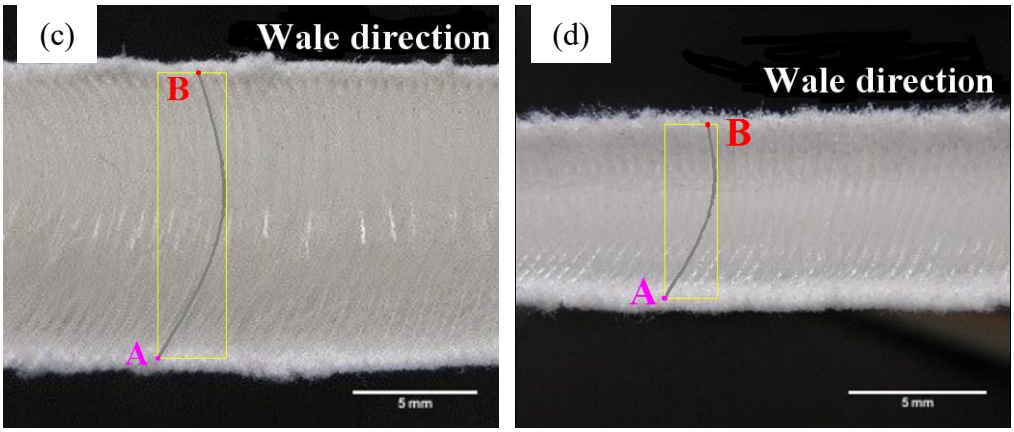

Figure 3 Cross-sectional views of spacer fabrics produced: (a) and (c) Spacer-20h; (b) and (d) Spacer-12h.

Fabric lamination

As mentioned before, all the monofilaments have a curved shape in the wale direction view. The formation of this shape mainly comes from the bending moments developed at the linking points by tuck loops. As shown in Figure 3(c) and 3(d), the linking points A and B for each monofilament are not located on the same vertical line in the fabric thickness direction. The main reason is that the courses where points A and B are located are not knitted simultaneously. As points A and B of each monofilament are not on the same vertical line, the transverse instability could take place along the wale direction when a single spacer fabric is subjected to a vibration test under a loaded mass. In order to circumvent the undesirable transverse shift along the wale direction of the spacer fabric structure during vibration tests, two identical spacer fabrics were bonded together using a double-sided adhesive tape as shown in Figure 4(a). Thus, point A and point C are located on the same vertical line. In this case, the topmost layer and the base layer of the laminated fabric can maintain opposite to each other under the mass loaded, as shown in Figure 4(b). As two fabrics are bonded together, the relative slip between two fabrics can be avoided. By this way, the transverse motion of the spacer fabric has no interference on the

vertical motion of the mass-spacer fabric system.

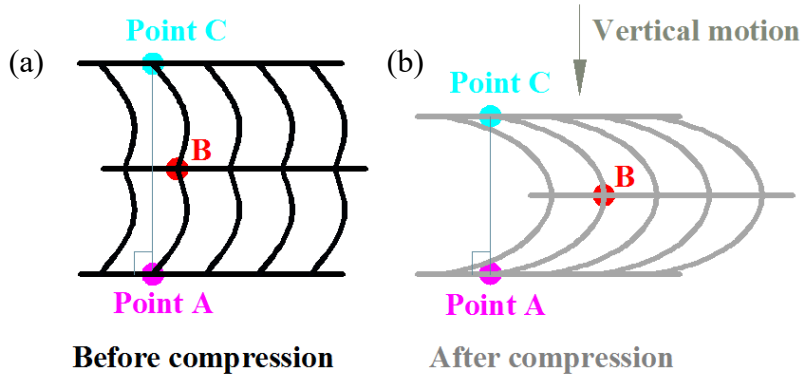

Figure 4 Schematic of fabric structure with two identical fabrics laminated together: (a) before compression; (b) under compression.

VIBRATION TEST

A vibration test system EM-400F3K-30N80 manufactured by the King Design Instrument Technology (Kun Shan) Co., Ltd was used to measure the vibration transmissibility of laminated weft-knitted spacer fabrics. The system mainly consists of an electromagnetic vibration shaker equipped with a vertically connected 35 cm × 35 cm square platform made of aluminum, a digital vibration controller VCS 102, a high power amplifier and protector, and a cooling blower. The schematic of the system is shown in Figure 5. The controller VCS 102 has one output channel (Output) and two input channels (Input 1 and Input 2), and generates voltage signals transmitted through the power amplifier to drive the shaker platform to vibrate at predefined frequencies and excitation levels. Then, acceleration signals measured by two accelerometers respectively mounted on the shaker platform (Accelerometer 1) and the load mass (Accelerometer 2) were sent back through Input 1 and Input 2 to the controller for data acquisition. It should be noted that Accelerometer 1, Input 1, Controller, and Output form a feedback control system to ensure that the shaker platform vibrates correctly according to the

predefined profile. The controller was also connected to the test software of PC for waveform display and analysis. The cooling blower cooled down the shaker for safety purpose.

The mounting of two accelerometers for measuring the acceleration transmissibility of the mass-spacer fabric system is shown in Figure 6. The spacer fabric to be tested is placed on the center of the shaker platform and top-loaded with a metallic mass. The accelerometer stud-mounted on the shaker platform was an accelerometer Brüel & Kjær 4514-004 with a sensitivity of 50.9 mV/g and an acceleration range of 100 g, where g is the gravitational acceleration (9.81 m/s^2). The other accelerometer PCB 352A56 with a sensitivity of 101.7 mV/g and an acceleration range of 50 g was adhesively mounted on the center of the load mass using petro wax.

The size of fabric sample and that of load mass were selected by referring to the International Standard BS EN ISO 13753:2008 [31]. According to this standard, the material to be tested shall contain a circular area of no less than 45 mm in radius; besides, the load block shall be a circular cylinder with a radius of 45 mm and a mass of 2.5 kg. However, due to the nearly orthotropic material properties of weft-knitted spacer fabric structure, it would be appropriate to have fabric samples cut into a square shape rather than a circular one. Consequently, spacer fabric samples used were cut into a size of 150 mm × 150 mm. In order to weaken the edge effect and avoid mass eccentricity, square steel blocks with a surface area smaller than that of spacer fabric samples (90 mm × 90 mm), but with different masses were used as the load masses.

The shaker was excited by sinusoidal sweeps from 4 Hz to 500 Hz with a sweep rate of 1.0 Oct/min. It should be noted that the sweep rate has an influence on the transmissibility behavior

of fabric. With a high sweep rate, the response of system may have not yet reached steady state before the driving frequency moves to the next magnitude. With a low sweep rate, however, the amount of time spent becomes greatly prolonged, thus bringing another problem which involves the fatigue and viscoelasticity of materials. Consequently, a compromise between both requirements for the sweep rate is needed to ensure the reliability of results. After a series of trials, it was found that a sweep rate of 1.0 Oct/min could ensure the reliability of results for this kind of knitted spacer fabrics. During each sweep process, the excitation level was kept constant. Three excitation levels, namely, 0.1 g, 0.2 g or 0.3 g, were selected. It should be noted that excitation amplitude decreased as the driving frequency increases. Five different load masses from 1 kg to 5 kg were used. Acceleration transmissibility values at desired frequencies were obtained during tests. Three replications were carried out for each testing condition.

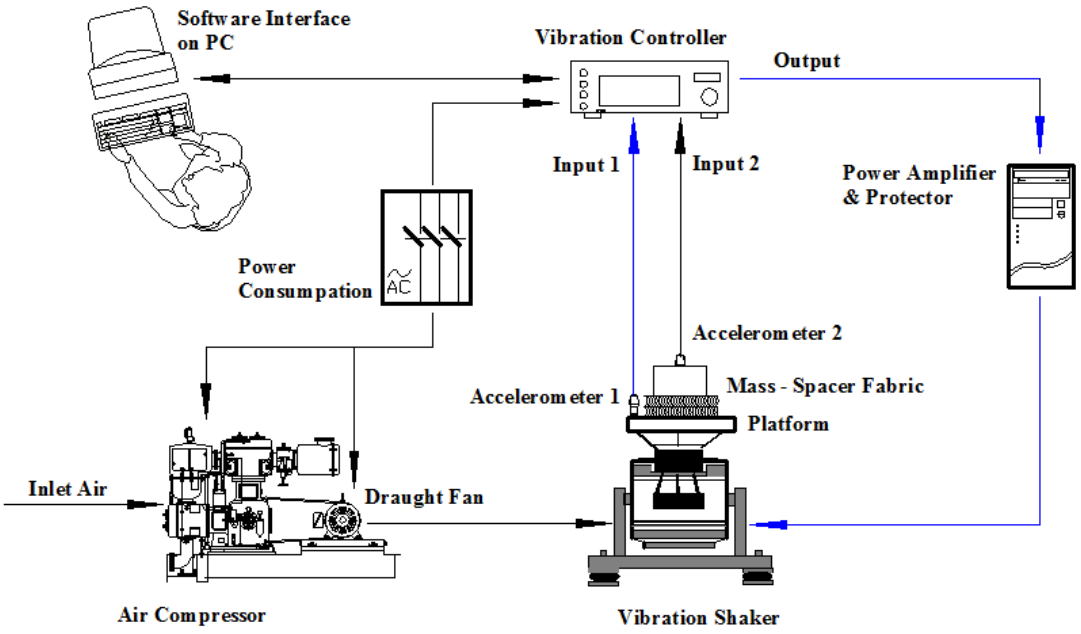

Figure 5 Schematic of the vibration testing system.

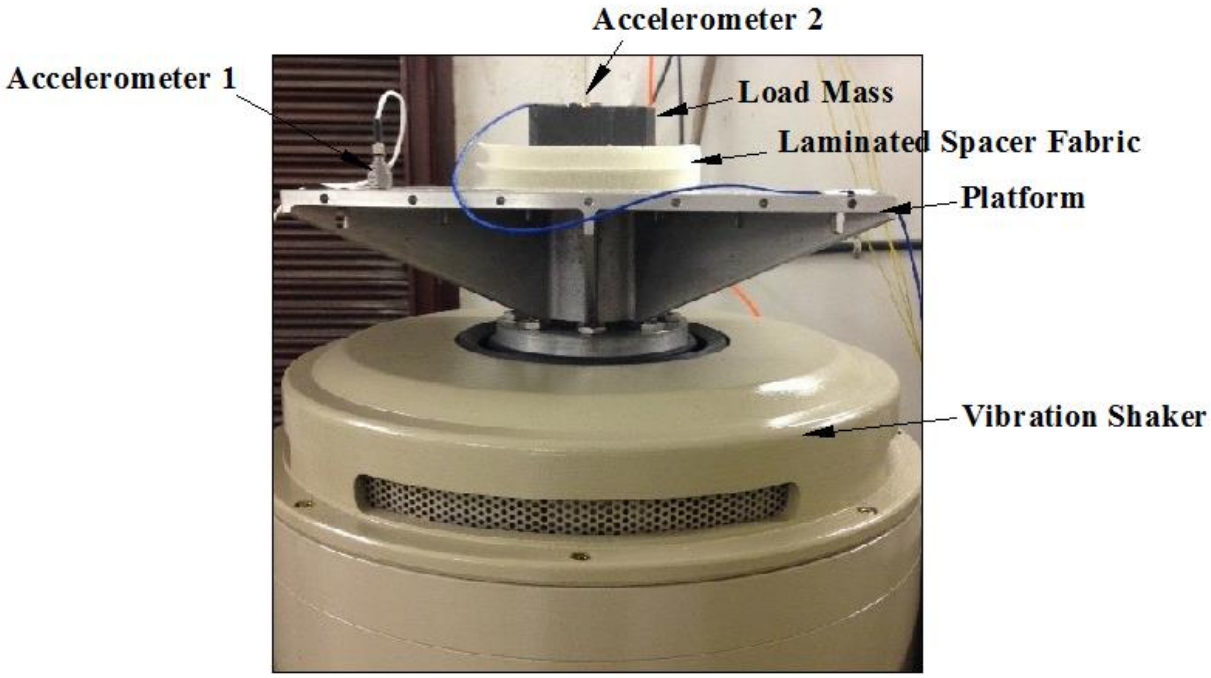

Figure 6 Photo of the mass-spacer fabric system and the mounting of two accelerometers.

QUASI-STATIC COMPRESSION TEST

In order to better understand how the nonlinear behavior of spacer fabrics affects the vibration isolation performance, a quasi-static compression test was also conducted for the laminated fabrics on an Instron tester 5566 installed with two compression platens. The compression speed was set as 12 mm/min and the maximum compression strain was chosen as 60% of the original fabric thickness. The sample size used was 90 mm × 90 mm, the same as that of load blocks.

RESULTS AND DISCUSSION

Typical transmissibility curve

The vibration isolation performance of the weft-knitted spacer fabrics was evaluated by the acceleration transmissibility T which is defined as the ratio of the acceleration of the load mass

to that of the shaker platform. As shown in Figure 7, a typical curve of T as a function of the excitation frequency obtained for Spacer-12h when tested under 0.3 g excitation level and 2 kg load mass is selected as an example to explain the vibration isolation performance of this type of spacer fabrics. Although the tests were conducted from 4 Hz to 500 Hz, all the acceleration transmissibility curves shown in afterwards are only until 100 Hz to get a better demonstration. From Figure 7, it can be seen that under low excitation frequencies, the acceleration transmitted from the platform to the mass approximately equals the excitation level. However, with increasing the excitation frequency, the transmissibility rapidly increases until the resonance peak. The transmissibility reading above one unit ($T>1$) indicates that the vibration is amplified. At resonance frequency f_r (15.2 Hz), the transmissibility of the mass-spacer fabric system reaches the peak value T_{max} (4.1). It means that acceleration is amplified by 4.1 times. Further elevating the excitation frequency above f_r, the transmissibility starts to decline. The frequency at which the transmissibility equals one unit ($T=1$) is called the crossover frequency f_c (30.3 Hz), which defines the boundary between the amplification region and the isolation region. Vibration isolation ($T<1$) takes effect when the excitation frequency is larger than f_c.

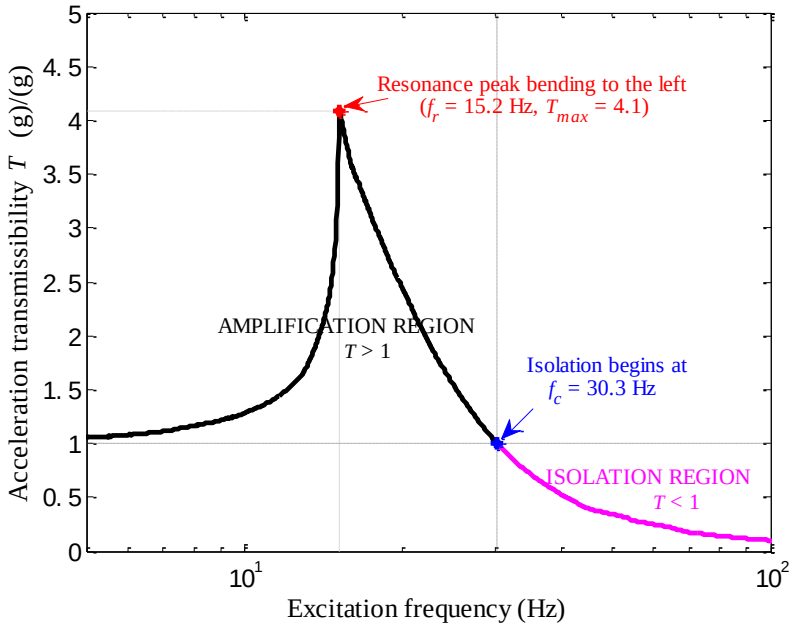

Figure 7 Typical acceleration transmissibility curve for Spacer-12h under 0.3 g excitation level and 2 kg load mass.

To achieve a wider isolation region, the resonance frequency f_r should be reduced. In a linear single-degree-of-freedom (SDOF) system, the curve shape near the resonance peak looks symmetric. In such a kind of system [32], f_r is related to the dynamic stiffness k_d and the load mass m, and is defined by equation $f_r = \frac{1}{2\pi}\sqrt{\frac{k_d}{m}}$. Observing the curve in Figure 7, it can be found that the curve shape near the resonance peak is asymmetric and bent to the left side, indicating that the mass-spacer fabric system is a nonlinear one. Although in a nonlinear system, the calculation of f_r becomes more complicated, f_r is still affected by k_d and m. Besides, under a low excitation level, such a mass-spacer fabric system can be assumed as a linear one. The reduction of f_r implies either decreasing k_d or increasing the load mass. Since the load

mass is predefined by the working condition, decreasing k_d should be the only approach to a better isolation performance.

Therefore, an ideal isolator should keep the dynamic stiffness as low as possible. However, due to the nonlinearity of weft-knitted spacer fabric, the value of k_d is affected by the load mass, the fabric thickness and the excitation level. For this reason, the following sections will discuss the effects of these factors on the isolation performance of the mass-spacer fabric system. For better comparison, two physical quantities, the resonance frequency f_r and the crossover frequency f_c, are selected. Since the amplification region is to be avoided during the use, the peak transmissibility T_{max} is not a concern in this study.

Effects of fabric thickness and load mass

Under the same excitation level, the effect of the fabric thickness on the vibration isolation performance also depends on the load mass due to nonlinear behaviors of spacer fabrics under both static and dynamic loading conditions. In other word, the spacer fabrics will be deformed at different compression strains and will have different stiffness when the load mass changes. In this regard, the effects of the fabric thickness and load mass are discussed together in this section. For ease of discussion, only the testing results for one excitation level of acceleration are presented here. The effect of the excitation level will be discussed in the next section.

Figure 8(a) and (b) respectively show the transmissibility curves of Spacer-20h and Spacer-12h with different load masses when the excitation level is kept at 0.1 g. It can be seen that the resonance peaks of the transmissibility curves shift to the left side when the load mass increases.

This implicates that f_r and f_c decrease with the increase of the load mass (Figure 8(c)). However, as shown in Figure 8(a), an exceptional case is found for Spacer-20h when the load mass increases from 4 kg to 5 kg. In this case, the transmissibility curve with 5 kg load mass shifts back to the right side instead of shifting to the left side, resulting in a slight increase of f_r and f_c as shown in Figure 8(c). When observing the effect of the fabric thickness, it can be found that f_r and f_c of Spacer-20h are smaller than those of Spacer-12h, indicating that f_r and f_c decrease with the increase of the fabric thickness.

(a)

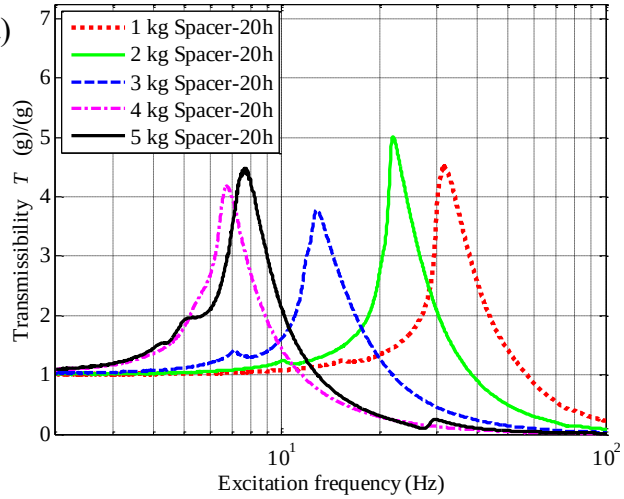

(b)

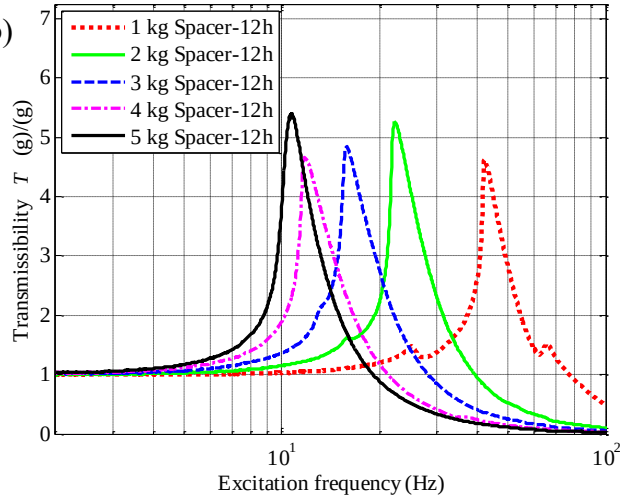

(c)

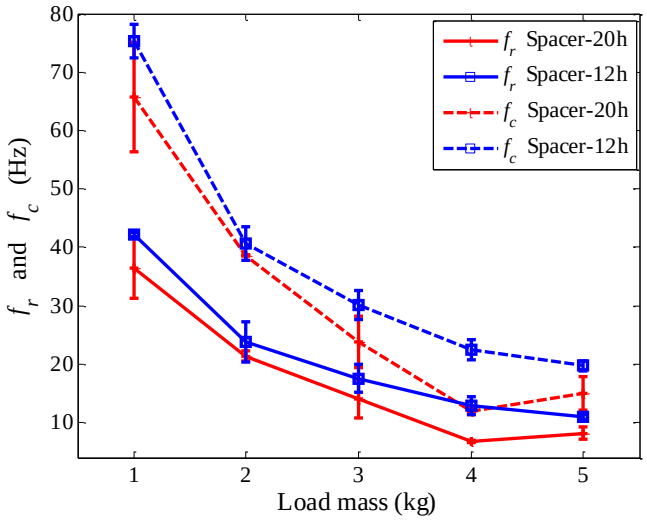

Figure 8 (a) and (b) Transmissibility curves under 0.1 g excitation level with load mass varied; (c) Variation of f_r and f_c with load mass.

The above phenomena can be explained by stiffness changes of spacer fabrics when the load mass changes. As shown in Figure 9, the quasi-static compression curves of both laminated Spacer-20h and Spacer-12h are nonlinear, which indicate that their static stiffness k_s cannot be kept constant under different compression loads. It can be seen that although the compression curves of two spacer fabrics are very different, the variation trends of their static stiffness k_s are very similar. This is that k_s first increases at the very beginning stage, then slightly decreases and finally rapidly increases due to the compaction of the fabric structure under high compression loads. However, the k_s values of two fabrics are different. It should be pointed out that under vibration condition, the dynamic stiffness k_d should be used to explain the vibration isolation performance of spacer fabrics. According to the quasi-static compression curves in Figure 9, it can be derived that the compression behavior of two weft-knitted spacer fabrics is similar to that of damping materials. Therefore, their dynamic stiffness k_d should be different from their static

stiffness k_s due to history-dependent mechanical properties under vibration condition. In spite of the nonlinear compressive force-displacement relationship of spacer fabrics, under 0.1 g excitation level, the vibration is so localized that the mass-spacer fabric system could be treated as linear. Using $f_r = \frac{1}{2\pi}\sqrt{\frac{k_d}{m}}$, the values of k_d for two spacer fabrics with five load masses were calculated and listed in Table 2. It can be seen that the k_d values of Spacer fabric-20h are lower than those of Spacer-12h. This explains why f_r and f_c decrease with the increase of the fabric thickness and the thicker spacer fabric has better vibration isolation than the thinner fabric.

The variation trends of k_d also explain why f_r and f_c decrease with the increase of the load mass because the k_d values also decrease with the increase of the load mass. The exceptional case for Spacer-20h, in which f_r and f_c increases when the load mass increases from 4 kg to 5 kg, can be also explained by k_d value change and static compression curve. As shown in Figure 9, when the load mass increases from 4 kg to 5 kg, Spacer-20h changes into the compaction stage with a rapid increase of stiffness. As the effect of the increase of stiffness is higher than that of the increase of load mass, f_r and f_c increases when the load mass increases from 4 kg to 5 kg. Table 2 also confirms that the k_d values increase when the load mass increases from 4 kg to 5 kg.

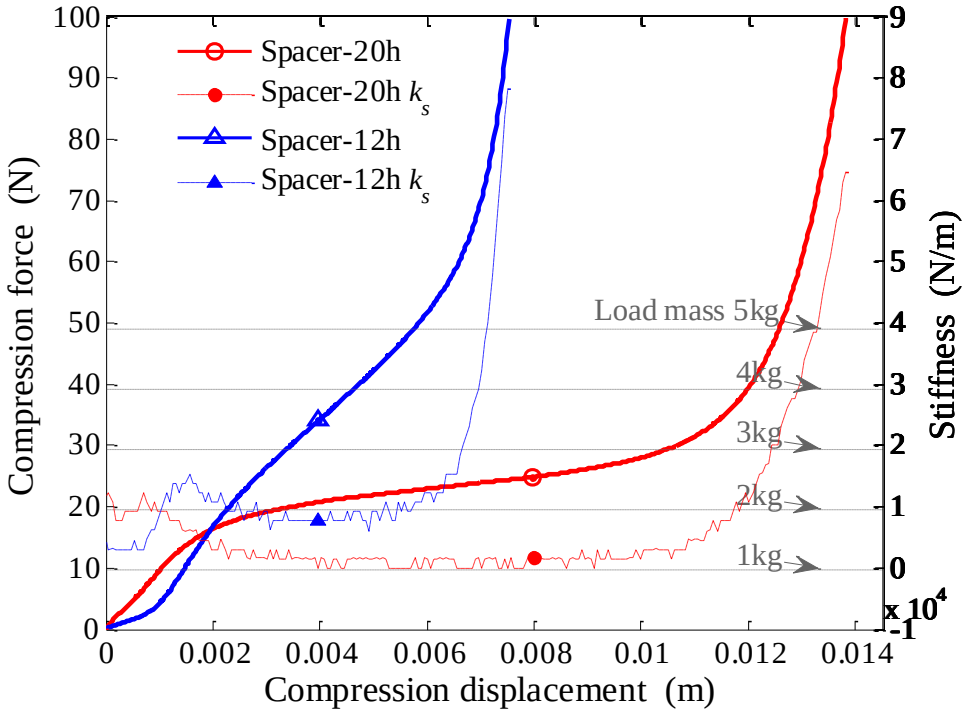

Figure 9 Quasi-static compression curves (solid line '—') and stiffness curves k_s (dashed line '- -') of spacer fabrics.

Table 2 k_d values of mass-spacer fabric system for a fixed excitation level at 0.1 g.

Load mass (kg)		1	2	3	4	5
k_d (×10^4 N/m)	Spacer-20h	5.26	3.69	2.32	0.74	1.32
	Spacer-12h	7.03	4.96	3.65	2.62	2.40

Effect of excitation level

The previous section discussed the effects of both the fabric thickness and load mass with a fixed excitation level. In this section, the effect of excitation level is discussed with a fixed load mass.

Figure 10(a) and (b) respectively show the transmissibility curves of Spacer-20h and Spacer-12h with different excitation levels when the load mass is kept at 2 kg. It can be seen that the resonance peaks of the transmissibility curves shift to the left side when the excitation level increases. This implicates that f_r and f_c decrease with the increase of the excitation level (Figure 10(c)). From Figure 10(a) and (b), it can be also found that the shapes of transmissibility curves at the resonance peaks get much bent to the left side when the excitation level increases, indicating that the mass-spacer fabric system becomes more softening. As the increase of softening implicates a decrease of the dynamic stiffness k_d, f_r and f_c decrease with the increase of the excitation level.

From Figure 10(c), it can be also found that the f_r and f_c values of Spacer-20h are lower than those of Spacer-12h for all the excitation levels, which confirms again that the thicker spacer fabric has better vibration isolation performance than the thinner spacer fabric. The result in Figure 10(c) also shows that the difference in f_r and f_c between two spacer fabrics increase with the increase of excitation level. The reason may be explained by the fact that at low excitation level, the dynamic loads applied to the fabric are relatively smaller and two fabrics work at their low deformation regions where the difference of their stiffness is not high. However, with increasing the excitation level, the dynamic loads applied to the fabric increase and two fabrics will work in different deformations regions where their stiffness gets more important. The detailed explanation needs a further theoretical analysis by considering the nonlinear softening of the mass-spacer fabric system, which is beyond the scope of this paper.

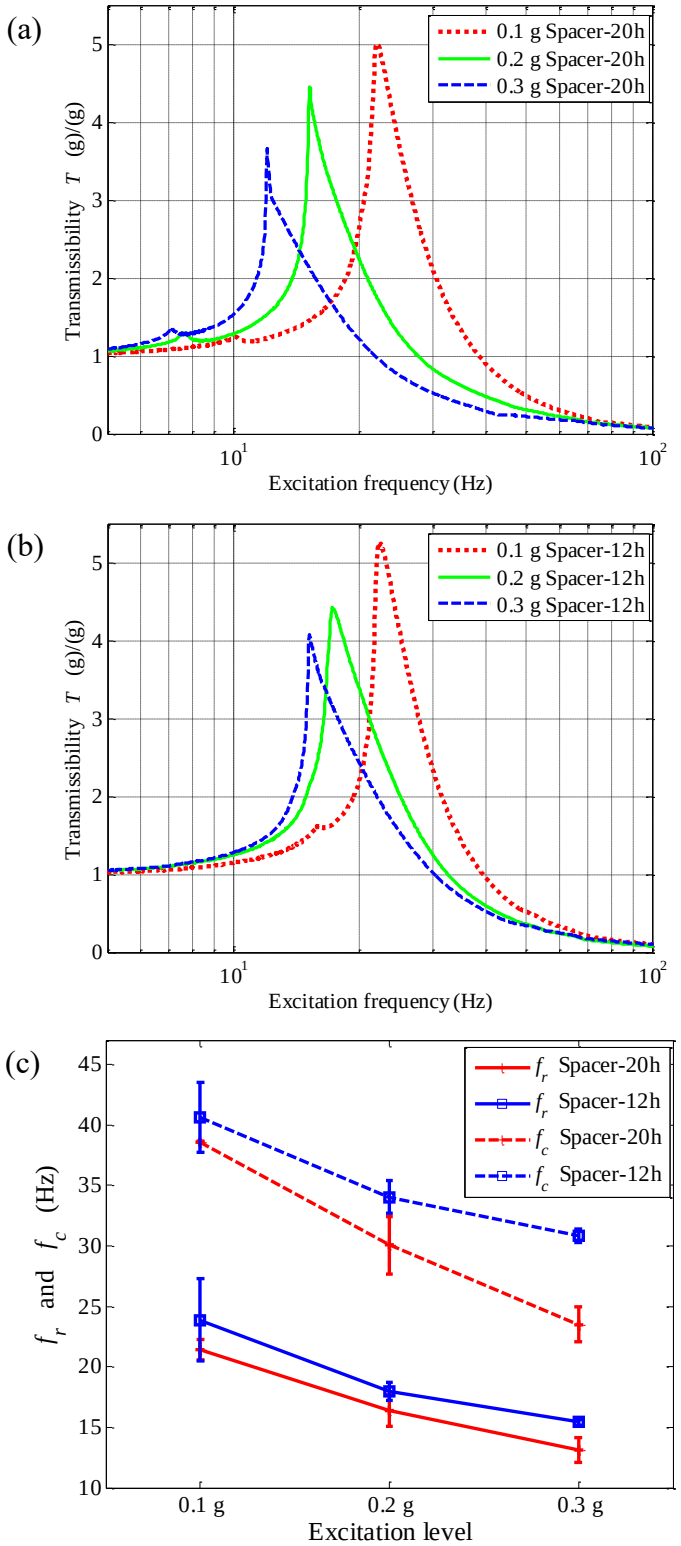

Figure 10 (a) and (b) Transmissibility curves under 2 kg load mass with excitation level varied; (c) Variation of f_r and f_c with load mass.

CONCLUSIONS

According to the results above obtained, the following conclusions can be drawn.

1) The vibration behaviors of weft-knitted spacer fabrics are not linear due to their nonlinear compression force-displacement relationships which result in different stiffness under different load mass and excitation level.
2) Increasing the fabric thickness can result in a decrease of the resonance frequency and crossover frequency due to reduction of stiffness, and thus improve the vibration isolation performance of spacer fabrics.
3) The higher load mass normally results in a smaller resonance frequency and a smaller crossover frequency. However, too high load mass makes fabric compacting, resulting in a higher resonance frequency and a higher crossover frequency due to a rapid increase of fabric stiffness.
4) Increasing the excitation level results in a smaller resonance frequency and a smaller crossover frequency, and thus a broadened frequency region for vibration isolation. The nonlinear effect gets more important when the excitation level increases.

It is expected that this study could promote the commercial application of weft-knitted spacer fabrics for the vibration isolation. By proper design of fabric structures, vibration risks in different working environments such as during transportation and hand arm vibration from operating hand-held power tools can be reduced. Moreover, this study can be extended to other textile structures for the anti-vibration purpose. Due to the great varieties of textile products, not only weft-knitted and warp-knitted spacer fabrics but also 3D woven and nonwoven fabrics can also be designed as vibration isolators.

Acknowledgement

The authors would like to acknowledge the funding support from the Research Grants Council of HK Special Administrative Region Government (Grant No. 516011).

REFERENCES

1. Griffin MJ. *Handbook of human vibration*. Academic press, 2012.

2. Deng R, Davies P and Bajaj AK. Flexible polyurethane foam modelling and identification of viscoelastic parameters for automotive seating applications. *Journal of Sound and Vibration*. 2003; 262: 391-417.

3. Joshi G, Bajaj AK and Davies P. Whole-body vibratory response study using a nonlinear multi-body model of seat-occupant system with viscoelastic flexible polyurethane foam. *Industrial Health*. 2010; 48: 663-74.

4. Jack RJ. The effectiveness of using two different types of anti-vibration gloves compared to bare hand condition at dampening the frequencies associated with hand-arm vibration syndrome. *Work (Reading, Mass)*. 2004; 25: 197-203.

5. Patten WN, Sha S and Mo C. A vibrational model of open celled polyurethane foam automotive seat cushions. *Journal of Sound and Vibration*. 1998; 217: 145-61.

6. Pereira S, Anand SC, Rajendran S and Wood C. A study of the Structure and Properties of Novel Fabrics for Knee Braces. *Journal of Industrial Textiles*. 2007; 36: 279-300.

7. Wollina U, Heide M and Swerev M. Spacer Fabrics–A Potential Tool in the Prevention of Chronic Wounds. *Exogenous Dermatology*. 2002; 1: 276-8.

8. Wollina U, Heide M, Müller-Litz W, Obenauf D and Ash J. Functional textiles in

prevention of chronic wounds, wound healing and tissue engineering. *Current Problems in Dermatology*. 2003; 31: 82-97.

9. Milosavljević S and Škundrić P. Contribution of textile technology to the development of modern compression bandages. *Chemical Industry and Chemical Engineering Quarterly*. 2007; 13: 88-102.

10. Tong S-f, Yip J, Yick K-l and Yuen C-wM. Exploring use of warp-knitted spacer fabric as a substitute for the absorbent layer for advanced wound dressing. *Textile Research Journal*. 2015; 85: 1258-68.

11. Dias T, Monaragala R, Needham P and Lay E. Analysis of sound absorption of tuck spacer fabrics to reduce automotive noise. *Measurement Science and Technology*. 2007; 18: 2657.

12. Dias T, Monaragala R and Lay E. Analysis of thick spacer fabrics to reduce automobile interior noise. *Measurement Science and Technology*. 2007; 18: 1979.

13. Funke HL, Gelbrich S, Ehrlich A, Ulke-Winter L and Kroll L. Anisotropic fibre-reinforced plastics as formworks for single and double-curved textile reinforced concrete. *Journal of Materials Science Research*. 2015; 4: 36.

14. Funke HL, Gelbrich S, Ehrlich A, Ulke-Winter L and Kroll L. Unsymmetrical Fibre-Reinforced Plastics for the Production of Curved Textile Reinforced Concrete Elements. *Open Journal of Composite Materials*. 2014; 4: 191.

15. Han F, Chen H, Zhang W, Lv T and Yang Y. Influence of 3D spacer fabric on drying shrinkage of concrete canvas. *Journal of Industrial Textiles*. 2014: 1528083714562087.

16. Han F, Chen H, Jiang K, Zhang W, Lv T and Yang Y. Influences of geometric patterns of 3D spacer fabric on tensile behavior of concrete canvas. *Construction and Building Materials*.

2014; 65: 620-9.

17. Stegmaier T, Linke M and Planck H. Bionics in textiles: flexible and translucent thermal insulations for solar thermal applications. *Philosophical Transactions of the Royal Society A: Mathematical, Physical and Engineering Sciences*. 2009; 367: 1749-58.

18. Liu Y, Au WM and Hu H. Protective properties of warp-knitted spacer fabrics under impact in hemispherical form. Part I: Impact behavior analysis of a typical spacer fabric. *Textile Research Journal*. 2014; 84: 422-34.

19. Liu Y, Hu H and Au WM. Protective properties of warp-knitted spacer fabrics under impact in hemispherical form. Part II: effects of structural parameters and lamination. *Textile Research Journal*. 2014; 84: 312-22.

20. Liu Y, Hu H, Long H and Zhao L. Impact compressive behavior of warp-knitted spacer fabrics for protective applications. *Textile Research Journal*. 2012; 82: 773-88.

21. Soin N, Shah TH, Anand SC, et al. Novel "3-D spacer" all fibre piezoelectric textiles for energy harvesting applications. *Energy & Environmental Science*. 2014; 7: 1670-9.

22. Wang Z and Hu H. A finite element analysis of an auxetic warp-knitted spacer fabric structure. *Textile Research Journal*. 2015; 85: 404-15.

23. Wang Z and Hu H. 3D auxetic warp-knitted spacer fabrics. *Physica Status Solidi (B)*. 2014; 251: 281-8.

24. Wang Z, Hu H and Xiao X. Deformation behaviors of three-dimensional auxetic spacer fabrics. *Textile Research Journal*. 2014; 84: 1361-72.

25. Chen F, Hu H and Liu Y. Development of weft-knitted spacer fabrics with negative stiffness effect in a special range of compression displacement. *Textile Research Journal*. 2015; 85: 1720–31.

26. Blaga M, Seghedin N-E and Ciobanu AR. Warp knitted fabrics behaviour under dynamic testing. *DE REDACTIE*. 2013: 334.

27. Blaga M, Seghedin N-E and Ciobanu AR. Weft knitted spacer fabrics response to vibrations. *14th AUTEX World Textile Conference*. Bursa, Turkey 2014.

28. Arabzadeh F, Sheikhzadeh M, Ghane M, Hejazi SM and Arabzadeh F. Mathematical modeling of spacer fabrics under impulsive loading. *Journal of the Textile Institute*. 2012; 103: 1031-41.

29. Liu Y and Hu H. Vibration isolation performance of warp-knitted spacer fabrics. *Fiber Society spring conference*. Hong Kong 2011, p. 63-4.

30. Liu Y and Hu H. Compression property and air permeability of weft-knitted spacer fabrics. *The Journal of the Textile Institute*. 2011; 102: 366-72.

31. BS EN ISO 13753:2008 Mechanical vibration and shock. Hand-arm vibration. Method for measuring the vibration transmissibility of resilient materials when loaded by the hand-arm system. BSI, 2008.

32. Carrella A, Brennan MJ and Waters TP. Static analysis of a passive vibration isolator with quasi-zero-stiffness characteristic. *Journal of Sound and Vibration*. 2007; 301: 678-89.